Topological Control of Triply Periodic Minimal Surfaces for Thermal Design and Advanced Manufacturing: A Gyroid Case Study

Vivek M. Rao[1], Jamieson Brechtl[2], Corson L. Cramer[3], Kashif Nawaz[2]

[1]Advanced Reactor Engineering and Development Section, Oak Ridge National Laboratory, 1 Bethel Valley Road, Oak Ridge, Tennessee 37830 USA
[2]Building Technologies Research Section, Oak Ridge National Laboratory, 1 Bethel Valley Road, Oak Ridge, Tennessee 37830 USA
[3]Composites Science and Technology Section, Oak Ridge National Laboratory, 1 Bethel Valley Road, Oak Ridge, Tennessee 37830 USA

Corresponding Author:
Vivek M. Rao
raovm@ornl.gov

Abstract:
Recently, triply periodic minimal surfaces have seen tremendous interest in the design of compact process engineering components. Benefits of high surface area per unit volume, modular form, and inherent periodicity provide a holistic self-supporting network and flow-conducive features. Applications of importance pertain to thermal power management, biomimetic scaffolds and structures, and feasibility of advanced manufacturing. This study presents a novel approach to the manipulation of the characteristic Schwarz-G, or 'gyroid' triply periodic minimal surface, for thermal design in the context of advanced manufacturing. The study presents relationships between design parameters and resulting surface area as a target response using the characteristic equation of a gyroid. Through parametric control, an approach to induce asymmetry in a gyroid is presented. Then, the characteristic equation is manipulated to produce a 20-fold increase in achievable area over a baseline design characteristic of 25.4 mm through controlled combinations of design parameters. A second relationship is presented as a function of the maximum area achieved and manipulated design parameters. Through the analysis, the study presents a framework to identify and maximize the achievable area of triply periodic minimal surfaces for advanced manufacturing and thermal management applications.

Keywords: Periodic, minimal, manipulated, gyroid, thermal, manufacturing

Abbreviations

TPMS	triply periodic minimal surface
CFD	computational fluid dynamics
3D	three-dimensional
CAD	computer aided design
ABS	acrylonitrile butadiene styrene
FDM	fused deposition modeling
LPBF	laser powder bed fusion

FEA	finite element analysis
sCO_2	supercritical carbon dioxide
HPC	high-performance computing
COP	coefficient of performance
PCHE	printed circuit heat exchanger

Symbols

dP	pressure differential
dP/L	pressure drop
Nu	Nusselt number
f	Fanning friction factor
Pr	Prandtl number

1. Introduction

The Schwarz-G, or gyroid is one of many triply periodic minimal surfaces (TPMSs), of significant mathematical interest since its discovery over fifty years ago [1]. In thermal engineering applications, a primary motivation behind is to leverage the high surface area-to-volume ratio, characteristic of TPMSs, in end applications of high loading; thermal, mechanical or hydraulic. In non-engineering applications, interest has stemmed from the ability to use scalable TPMSs to generate biomimetic structures and the use of advanced manufacturing techniques to fabricate prototypes. To manufacture a gyroid with suitable manufacturing tolerances, a CAD model must be developed through volumetric quantification of solid parts and voids for fluid flow. An example of such a realization of gyroids of different sizes and materials using fused deposition modeling (FDM) (at Oak Ridge National Laboratory (ORNL)) is shown in Figure 1.

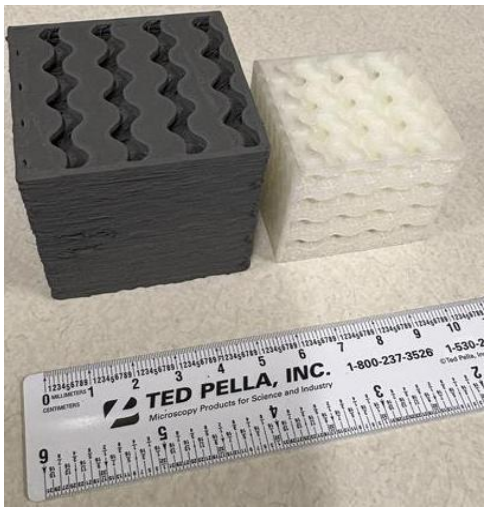

Figure 1. Gyroids of cubic edge length 50 mm (left) and 40 mm (right) printed at the Manufacturing Demonstration Facility located in ORNL.

Mathematical approaches to describing a typical gyroid have seen repeated attempts. In 1996, the construction and characterization of the gyroid surface with constant mean curvature was presented by Große-Brauckmann and Meinhard [2]. Using the characteristic equation of a

gyroid, a mathematical approach was later shown to relate a practical gyroid structure to surface design parameters [3]. The inherent periodicity of unit cells in sample structures coupled with symmetry of volumes separated by the gyroid make it an attractive option as a static mixer for fluid flow applications. One study pursued molecular and atomic scales of study to explore nineteen distinct gyroid nanostructures [4]. Of nineteen, three types were identified as ground-state structures corresponding to a given number of atomic-scale cycles, with asymmetry in the unit cell. Concurrently, a porosity-based approach gained traction in the description of void spaces created by a gyroid of finite wall thickness generated in a cubic template [5].

The Taguchi method has been pursued in some studies to control print parameters for TPMSs such as gyroids with finite wall thicknesses. In one study, a Taguchi L9 array was developed for the FDM of primitive and gyroid surfaces, where the primitive surface exhibited superior absorption energy and lower vibration than the gyroid [6]. In a similar study, the layer height, printing speed, and line width were studied via the Taguchi method to determine optimal settings for maximized energy absorption under compression in gyroids (layer height of 20 mm) and maximized strength of the diamond TPMS (layer height of 0.10 mm) at a print speed of 60 mm/s and line width of 0.40 mm [7]. Targeted closer to thermal management applications, gyroids with wall thicknesses of 0.2 mm, 0.5 mm and 0.7 mm were fabricated, using LPBF, for unit cells with sizes ranging from 10 mm to 12 mm [8]. The results revealed that samples with wall thicknesses of 0.5 mm or lower did not pass leakage tests.

Further increases in heat transfer are sought through smooth finishes of fabricated prototypes. In one study, recursive characterization was performed on gyroids that underwent abrasive jet polishing in which a correlation between Nu and f was determined for the as received and polished (smoothed) samples [9]. Additionally, fundamental studies of fluid flow and heat transfer in gyroids, as enhanced heat exchangers, have been studied with the objective of producing enhanced heat transfer area in compact footprints [8-11]. These studies examined the effects of various unit cell sizes, wall thicknesses, and porosity values. One study found that for a simple gyroid sheet structure, the porosity was the only factor to have a significant effect on thermal power, with a maximum thermal power recorded at 45% porosity [10]. A simple study compared a gyroid unit cell, a unit cell array, and a recursive gyroid structure to illustrate ways to enhance heat transfer area while correlating dP to f [11]. In a tubular volume, a gyroid was inscribed as a static mixer to study basic fluid flow and heat transfer characteristics [12]. Here, the authors introduced an additional term, which provided a deviation of local X and Y coordinates across the X-Y cross-section of a cylindrical containment, to generate gyroids of different thicknesses. Their results showed that this geometry resulted in a greater than 60% reduction in pressure drop and over 240% increase in the heat transfer rate as compared to a heat exchanger with conventional circular tubes of diameter equivalent to the length of the gyroid unit cell. In another study, a cold plate heat exchanger design was improved by incorporating optimized gyroid topologies (improved by varying their wall thickness and aspect ratio) to minimize pressure loss and temperature gradients [13]. The findings indicated that in the optimized gyroid design, there was a 7% increase in thermal power, 40% increase in thermal efficiency, and 61.5% decrease in pressure differential over the baseline. The effects of fundamental variations in the periodicity (number of turns per unit cell) and consequent changes in porosity (through the Darcy-Forchheimer framework) on the ratio dP/L, in incompressible laminar flow, was performed in [14]. The study revealed a specific correlation between Nu and Re when varying Pr from 0.7 to

14, which can be used to design fluid stream hydraulics and inflow conditions. A detailed optimization study showed that increasing wall thickness and/or smaller pore diameter or pattern length leads to enhanced thermal performance of the heat exchanger [15]. A similar investigation on thermal process parameters, such as stream inflow velocity and temperature, showed high velocities at gyroid corners and their effects on Nu and Re in aeroengines [16]. This study, however, did not consider the effects of compressibility on thermophysical properties which suggested that computational predictions could be improved for greater numerical accuracy in mass conservation and flow field resolution. In another aerodynamics study, it was shown that multi-morphology TPMS structures could be integrated through a sigmoid function to tradeoff a 8-12% increase in thermal power and 9-13% greater Nu for a 12-17% increase in friction coefficients [17]. A similar observation in parametric tradeoff was observed during analysis of gyroid structures for indirect evaporative cooling [18]; here, a lower COP was observed than in the conventional design due to a higher dP resulting from the flow path among dense unit cells but the greater surface area also provided higher heat removal.

As recent studies have proposed numerous correlations between Nu and Re under differing thermal and hydraulic operating conditions, some studies have focused on predicting the heat transfer coefficient and hydraulic diameter when the gyroid lattice is manipulated through primitive controls [19] and fitted with planar, finned structures for additional heat transfer enhancements [20]. These efforts are of significance as compact heat exchangers are designed for high-pressure fluids such as sCO_2 to operate at high temperatures (500°C and above) in pursuit of power cycles capable of higher than conventional efficiencies. In one investigation, diamond and gyroid structures were evaluated against a PCHE for sCO_2 operation with both structures outperforming the PCHE, but at the cost of a higher dP/L and consequently increased pumping power [21].

Based on these studies, the present investigation aims to fill the gap in knowledge regarding the manipulation of the gyroid lattice with parameters beyond the unit cell size, wall thickness, and porosity. The presented approach presents additional parameters which allow the gyroid to grow within a fixed size of unit cell, while exploring the effect of the iso-value surface on surface area of gyroid sheets. The outcome of this study is to enable near-term rapid prototyping and testing of gyroids with unprecedented surface area per volume for previously explored unit cell sizes.

2. Theory and Calculation

2.1. Theory

The characteristic equation of a gyroid is a surface of zero thickness when the characteristic equation is evaluated as $f(x, y, z) = 0$. The characteristic equation is given as Eq. (1) [22]:

$$\sin(x)\cos(y) + \sin(y)\cos(z) + \sin(z)\cos(x) = f(x, y, z) \quad (1)$$

For visualization, Eq. (1) is plotted over a cubic volume of edge length 10.2 cm (4 in.), as shown in Figure 2; in (a), Eq. (1) is shown over surfaces of the cubic volume, and in (b), Eq. (1) is plotted within the volume of the cube. The function, *f*, is continuous through zero and symmetric about zero.

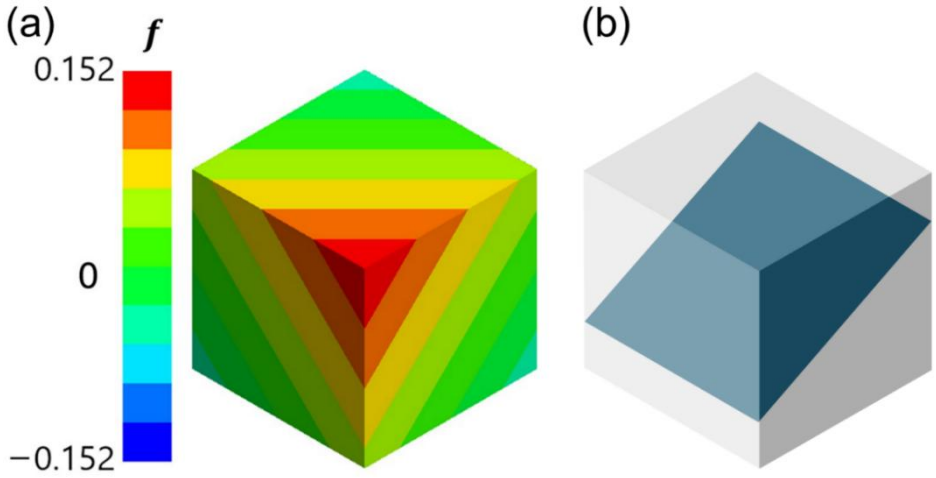

Figure 2. Gyroid representations based on Eq. (1): (a) plotted on surfaces of a cubic volume, and (b) iso-value surface of $f = 0$ within a cubic volume.

To develop control over the surface in a finite volume, Eq. (1) is presented in a parametric form in Eq. (2) to include the scaling of the x, y, and z coordinates with specific wavenumber multipliers (n, π, L):

$$sin\left(n_X\pi\frac{x}{L_X}\right)cos\left(n_Y\pi\frac{y}{L_Y}\right)+sin\left(n_Y\pi\frac{y}{L_Y}\right)cos\left(n_Z\pi\frac{z}{L_Z}\right)+sin\left(n_Z\pi\frac{z}{L_Z}\right)cos\left(n_x\pi\frac{x}{L_X}\right)=f(x,y,z) \quad (2)$$

where L_X, L_Y, and L_Z are length-scale parameters which can be set equal to the edge length of the cube. Additionally, the terms n_X, n_Y, and n_Z control the number of repetitions of scaled 'unit cells' along the X, Y, and Z axes, and in this paper, are assumed to be of a constant value, n.This approach has been adopted in numerous studies; for instance, in one recent study, disparate values of n_X, n_Y, and n_Z were used to vary the aspect ratio of the unit cell and study the effect of aspect ratio on thermo-hydraulics [10]. In another recent study, n was set equal to 2 while the thickness of the surface was varied to study the effect of infills on effective yield strength [13].

Figure 3(a) illustrates Eq. (2) plotted over surfaces of a cube with an edge length of 101.6 mm (4 in.). Figure 3(b) shows the iso-value surface at $f = 0$ within the cubic volume. Such theoretical representations are first generated in CAD models prior to thickening walls for realistic prototyping and testing.

From Figure 3, it is inferred that the control volume in which Eq. (2) is plotted generates two volumes separated by the gyroid surface. At $f = 0$, the two volumes are of equal magnitude; otherwise, the disparity in volume grows as the absolute value of f increases from zero. It is also observed that the area of the iso-value surface at non-zero values of f is lower than that at $f = 0$. Therefore, for the use of gyroids in heat transfer applications, it is suggested that exploration of designs at $f = 0$ will provide the greatest values of area, and consequently, greatest thermal

performance per unit volume. At non-zero values of *f*, asymmetric volumes are formed around the iso-value surface. The magnitude of asymmetry increases with respect to the absolute value of *f*. As the *f* approaches 1.2, the iso-value surface becomes discontinuous. Illustrations of gyroid surfaces with *f* values of 0, 0.3, 0.6, 0.9 and 1.2 are shown in Figure 4.

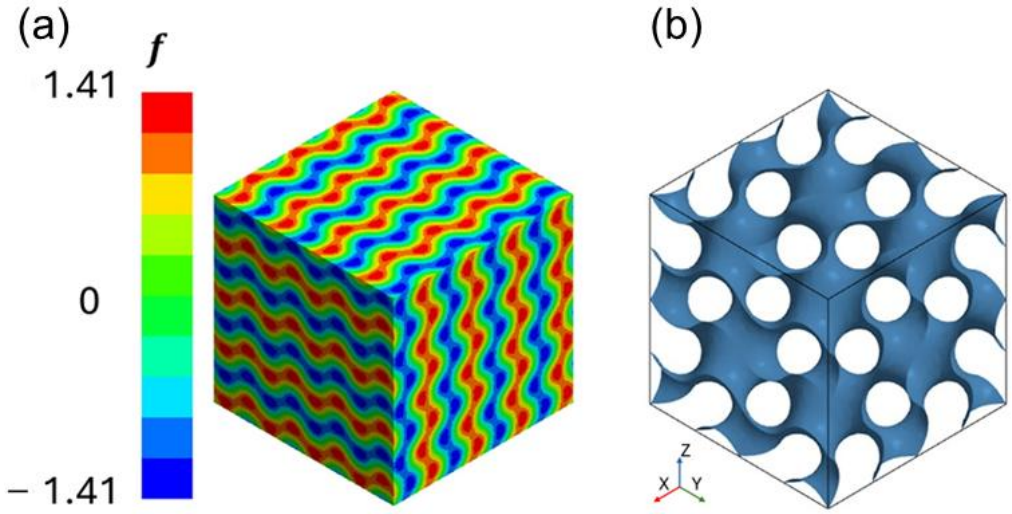

Figure 3. Gyroid surfaces derived from iso-value surfaces of Eq. (2), over surfaces of a cube with an edge length of 101.6 m (4 in.) (a) $f(x, y, z)$ plotted over surfaces of the volume and (b) $f = 0$ plotted within the volume.

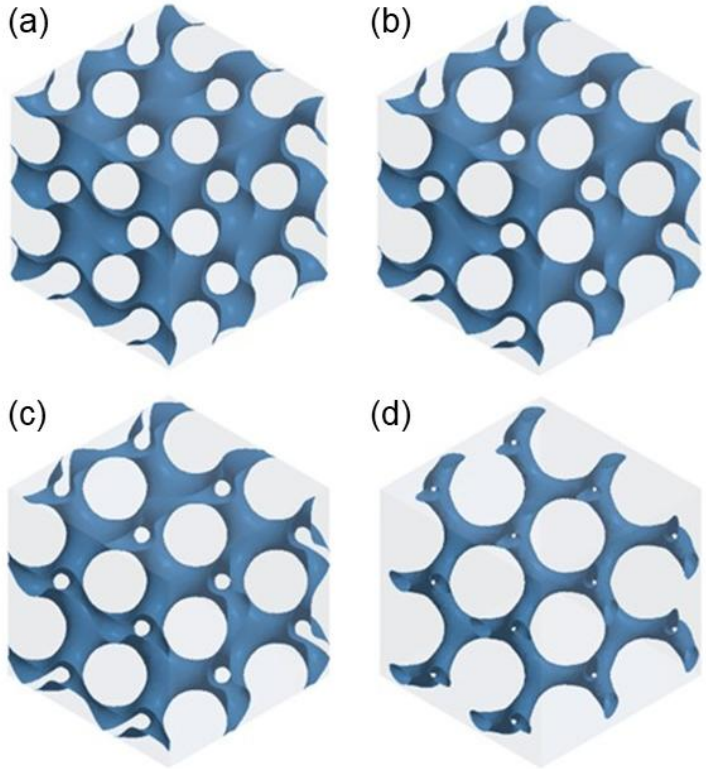

Figure 4. Decreasing surface area of iso-value surfaces with *f* values of (a) 0.3, (b) 0.6, (c) 0.9, and (d) 1.2.

At $f = 0$, it is desired to introduce local growth of unit cells to maximize the area of the iso-value surface. Parameters p_X, p_Y, and p_Z are introduced as exponents of the coordinates x, y, and z to allow Eq. (2) to be re-written as Eq. (3):

$$sin\left(\frac{n_X\pi}{L_X}\,x^{p_X}\right)cos\left(\frac{n_Y\pi}{L_Y}y^{p_Y}\right)+sin\left(\frac{n_Y\pi}{L_Y}y^{p_Y}\right)cos\left(\frac{n_Z\pi}{L_Z}z^{p_Z}\right)+\ sin\left(\frac{n_Z\pi}{L_Z}z^{p_Z}\right)cos\left(\frac{n_X\pi}{L_X}x^{p_X}\right)=f(x,y,z)=0 \quad (3)$$

For the sake of simplicity, p_X, p_Y, and p_Z are assumed to be of equal value, p. When $p = 1$, Eqs. (2) and (3) are identical. When $p < 1$, the smallest unit cell is formed where the $x, y,$ and z values are at their minimum. When $p > 1$, the smallest unit cell is formed when these values are at their maximum.

To the best of the authors' knowledge there is little, if any, work that has examined how exponentiating the independent variables of Eq. (2) affects the topological character of the gyroid. Thus, this paper aims to elucidate the effects of varying p in Eq. (3) to generate gyroids with constant wall thickness but varying surface area within each unit cell. Such an approach is expected to maximize the gyroid surface area within a given volume while including growth and shrinkage of the underlying gyroid for thermal management applications.

2.2. Calculation

To explore the topology of gyroid surfaces generated at different values of p, commercial software Simcenter Intelligent Design Exploration (IDE) [23] is used to conduct a rapid sweep of design parameters and identify the topology with maximum surface area. SC-IDE natively couples with Simcenter STAR-CCM+ (StarCCM) [24] and provides seamless integration of design, parameters, and solution space for rapid exploration. In StarCCM, the parameters are set up such that any changes are directly implemented in the generation of iso-value surfaces over a range of values designated for f and p. The current study is carried out in three stages. The first stage conducts a preliminary analysis to establish the variation in area due to linear changes in scaling parameter, L, and number of unit cells, n. The second stage investigates the effect of $1 \leq p < 2$ and $n = [1,2,3]$ at a fixed value of L. The third stage explores the effect of $0 < p < 1$ to complete the search space and identifies a global maximum for area of iso-value surface, $f = 0$. In IDE, performance ranking is developed by providing equal weight to all parameters and setting the objective to maximize the area of the iso-value surface.

The first two stages were completed directly in StarCCM on a workstation with a Windows 10 operating system and Intel ® Xeon® W-2123 CPU processor with clock speed of 3.6 GHz. The third stage was conducted on a high-performance computing (HPC) cluster with a Linux operating system, Rocky Linux 8.8, and AMD EPYC 9654 processors with dual-socket, 96 CPU cores and a clock speed of 2.40 GHz. The HPC cluster was used to generate a finite-volume mesh and report 4,000 values of area for iso-value surfaces of the gyroid based on parameter values using 192x CPU cores for 192 concurrent simulations. One time-step was simulated to generate the area of the iso-value surface.

3. Results and Discussion

In the first stage, a preliminary trend is established between the area of the iso-value surface and changes in n and L for $p = 1$. Here, the term 'iso-value surface' refers to the surface generated at $f = 0$. In the second stage, the effect of $1 \leq p < 2$ is discussed. In the third stage, exploration of surfaces at $0 < p < 1$ resulted in identification of the p value at which the area reaches a maximum above $p = 1$, and detailed discussion follows on identification of the greatest value of area using a combination of $f, p,$ and L.

3.1. Stage 1: Preliminary Study of Gyroids with $p = 1, f = 0$

Based on Eq. (3), it is evident that for $p = 1$, the argument inside the sine and cosine functions are dependent not only on the parameters n and L, but also on the spatial coordinates corresponding to (x, y, z). The resulting value of the function, f, ranges from -1.499 to 1.499. At $f = 0$, the iso-value surface evenly divides the volume in which f is plotted. In contrast, non-zero values generate asymmetry. It is seen that increasing n from 1 to 3 increases the area of the iso-value surface. Greater values of area are observed at lower values of L and higher values of n. Table 1 summarizes the relative changes in area of the iso-surface as n increases from 1 to 3 for fixed values of L. It can be observed that the increment in area over $n = 1$ is proportional to the change in n and is consistent for all values of L. The reference volume used in Table 1 is approximately 0.0011 m^3 for a cube of edge length 0.1016 m.

Table 1. Variation of area per unit volume with n and L at $p = 1, f = 0$.

	True area per unit volume (1/m)			Increment over $n = 1$		
n	$L = 0.0127\ m$	$L = 0.0254\ m$	$L = 0.0508\ m$	$L = 0.0127\ m$	$L = 0.0254\ m$	$L = 0.0508\ m$
1	121.78	60.88	30.44	1.0000	1.0000	1.0000
2	243.82	121.78	60.88	2.0021	2.0005	2.0002
3	366.41	182.75	91.32	3.0087	3.0020	3.0005

The values in Table 1 focus on rigid changes to the number of unit cells, n, or the length of each unit cell, L, to increase the area of the iso-value surface. From Figure 5, it can also be visually verified that the topology is scalable with respect to the ratio n/L. Therefore, the scope of thermal applications may range from a few millimeters, such as those encountered in micro-electronics and data center applications, to several meters as encountered in industrial heat transfer equipment. The inherent scalability of geometry lends itself to advanced manufacturing techniques for rapid prototyping at laboratory-scale as well as the elevation of technological maturity from conceptual prototype to demonstration in relevant environments. Symbiotically, this computational exercise can promote the maturity of manufacturing technologies and allow for feasible fabrication of complex topologies in thermal management systems at scales relevant to industry.

In Figure 5, the reader may proceed row-wise from (a)-(c), (d)-(f) and (g)-(i) to observe the increase in area of unit cells at a fixed number of unit cells per distance, L. Increasing L from 0.0127 m to 0.0254 m and 0.0127 m to 0.0508 m create 4-fold and 16-fold increases in the area of each unit cell, respectively. At each L, increasing the number of unit cells from 1 to 3 reveals a greater density of unit cells owing to three-dimensional spans in a cubic volume; therefore, an

increase in number of unit cells from 1 to 2 and 1 to 3 create an 8-fold and 27-fold decrease in the volume of each unit cell, respectively. This may be visually assessed column-wise in Figure 5 along (a)-(d)-(g), (b)-(e)-(h) and (c)-(f)-(i). Thus, rigid manipulation of the gyroid can create desired changes in area or volume, as a global phenomenon. This feature is leveraged in subsequent sections of this study to create localized changes in the unit cells.

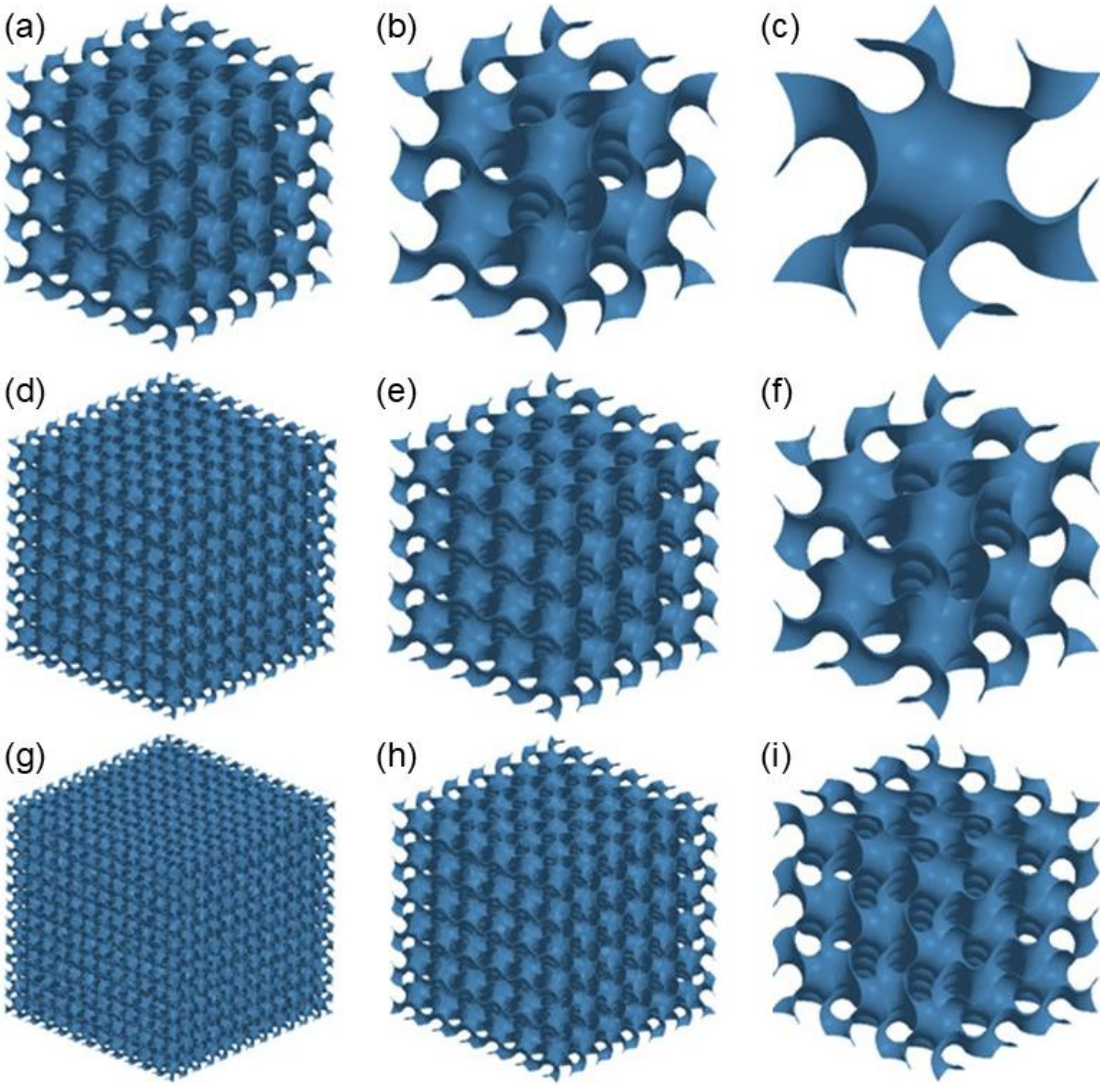

Figure 5. Illustrations of gyroid surfaces generated using values of n and L in Table 1: (a) $n = 1$, $L = 0.0127$ m, (b) $n = 1$, $L = 0.0254$ m, (c) $n = 1$, $L = 0.0508$ m, (d) $n = 2$, $L = 0.0127$ m, (e) $n = 2$, $L = 0.0254$ m, (f) $n = 2$, $L = 0.0508$m, (g) $n = 3$, $L = 0.0127$ m, (h) $n = 3$, $L = 0.0254$ m, and (i) $n = 3$, $L = 0.0508$ m.

3.2. Stage 2: Gyroids with $p \geq 1, f = 0$

When values of p were increased above 1, two salient observations were made. First, at a given value of p, the area of the iso-value surface increased proportionately with respect to n; this behavior is consistent with trends presented in Sec. 3.1. Second, as p increased, the area of the iso-value surface decreased for a given L and n. Variations in area and relative increments are summarized for $p \geq 1$ in Table 2. This decrease is consistent across values of *L* and *n* ranging from 0.0127 m to 0.0508 m and 1 to 3, respectively.

Table 2. Variation of area per unit volume with n and p at $f = 0$ and $L = 0.0127\ m$.

	True Area per Unit Volume (1/m)				Increment Over $n = 1$			
n	$p = 1.00$	$p = 1.25$	$p = 1.50$	$p = 1.75$	$p = 1.00$	$p = 1.25$	$p = 1.50$	$p = 1.75$
1	121.78	69.11	38.69	22.85	1.00	1.00	1.00	1.00
2	243.82	138.72	79.49	46.09	2.00	2.01	2.05	2.02
3	366.41	208.16	119.03	70.13	3.01	3.01	3.08	3.07

From the data in Table 2, the area per unit volume of each iso-value surface, A, was then normalized by the maximum value of area per unit volume in the range explored, A_{MAX}, and a correlation with p was found using a second-order polynomial fit, as given by the following equation:

$$A/A_{MAX} = 1.2098p^2 - 4.4017p + 4.1888 \tag{4}$$

Here, the scaled value of the iso-value surface area, A/A_{MAX}, is normalized for $n = 1$ and $p = 1$ for a given L. Thus, values of p greater than 1 will produce values of A/A_{max} less than 1. Iso-value surfaces of gyroids at $p = [1.25, 1.50, 1.75]$ are shown in Figures 6(a)-(c), respectively.

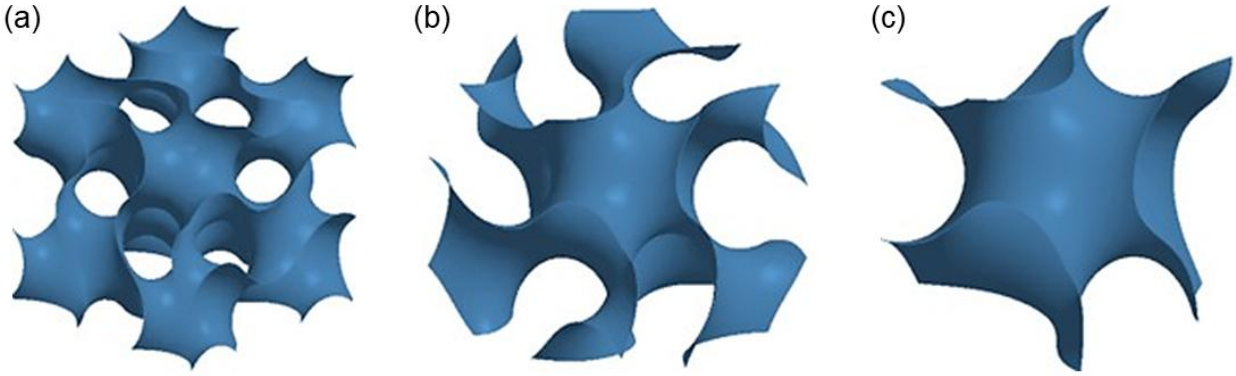

Figure 6. Iso-value surfaces of gyroids at $p > 1$, (a) $p = 1.25$, (b) $p = 1.50$, and (c) $p = 1.75$.

3.3. Stage 3: Exploration of Design Optimum for Maximum Area ($p < 1, f = 0$)

Further investigation into p values which could generate larger iso-value areas were pursued by exploring combinations of $p < 1$ and $f = 0$ over unit cells sizes ranging from 0.003175 m to 0.0254 m (in 0.003175 m increments)**.** These lengths were chosen in the context of conventional heat exchanger sizes. Figure 6 shows the effect of concurrent variation of p and f on the iso-value surface area. From Eq. (3), it is seen that for a given n, f, and p, lower values of L will give larger values of argument in the sine and cosine terms. At n = 1, it is seen from Figure 7 that the area gradually increases as p reduces from 1 to 0.3 and then sharply decreases as p reaches zero. This behavior suggests that an inflection point exists at or around $p = 0.3$, and can serve as a basis for further detailed optimization. Additionally, this behavior suggests that the framework of analysis could be extended to other TPMSs, such as the Schwarz-P or Schwarz-D for example. In the context of prototype manufacturing for thermal management applications, it may be noted that the range of unit cell sizes studied can be refined to a reference size of 3.175 mm ("best design") to develop iso-value surface areas roughly 20 times as large as those at the initial reference size of 25.4 mm ("baseline design") at $f = 0$. No increase in area was seen at values of $f > 0$.

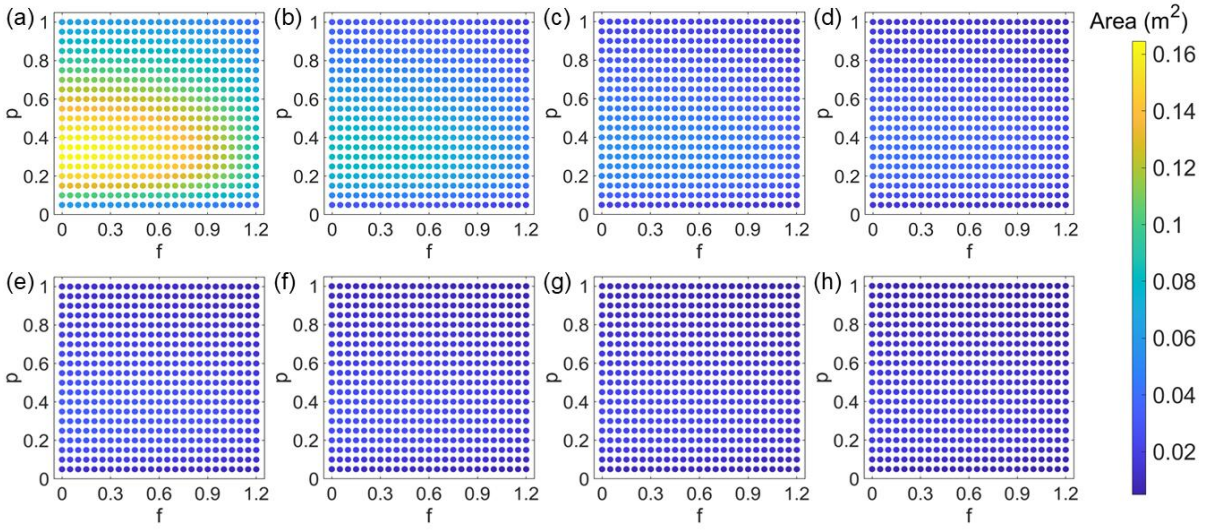

Figure 7. Variation of area with concurrent variation of f and p at (a) $L = 3.175\ mm$ (b) $L = 6.35\ mm$ (c) $L = 9.525\ mm$ (d) $L = 12.7\ mm$ (e) $L = 15.875\ mm$ (f) $L = 19.05\ mm$ (g) $L = 22.225\ mm$ (h) $L = 25.4\ mm$.

Figure 8 features a connectivity plot of L, f, p, and area (A) of the iso-value surface. Here, a parametric sweep of 4,000 combinations was explored with the area of iso-value surface ($f = 0$) as the response. The best design, which is highlighted by the red line in the figure, exhibits the largest area due to the smallest unit cell size. Compared to the baseline design (black line in the figure) with a unit cell size of 25.4 mm, the best design uses a unit cell size of 3.175 mm, or 1/8th the baseline value. Therefore, it is possible to harness more area in the same volume by altering not only the value of L and n, but also varying the size of individual unit cells through the value of p.

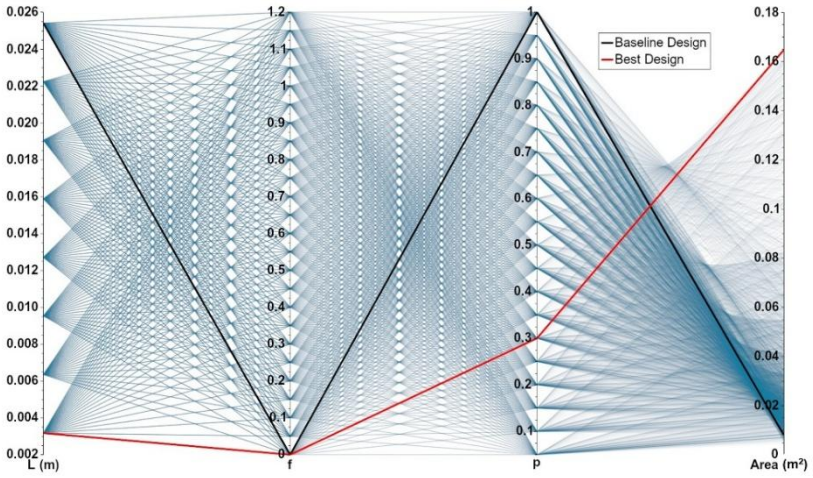

Figure 8. Connectivity plot of L, f, p, and area (A) of iso-value surface.

At $p = 0$, the area generated is near-zero. Therefore, a low, non-zero value of 0.05 is used as a minimum. An evaluation of the area generated on the iso-value surface at $f = 0$ by variation of p from 0.01 to 1 shows the lowest value at $p = 0.01$, and the maximum value at $p = 0.3$. At $p = 1$, the area is lowest observed over the range of interest from p. A fourth-order polynomial fit provides the relationship between scaled area, $\frac{A}{A_{MAX}}$, and p as:

$$\frac{A}{A_{MAX}} = -7.7312p^4 + 21.594p^3 - 21.599p^2 + 8.0239p + 0.033 \quad (5)$$

Using computational methods, it is observed that Eq. (5) approaches a maximum at $p = 0.3048$. However, using the p values from this study a trend of the area, as scaled by the maximum value at $p = 0.3$, is shown in Figure 9. Further analysis of the data found that the root mean square error (RMSE) was 0.01, indicating that the equation is a good fit to the data. The true value of maximum corroborates the approach in this study to explore values of p less than 1 to maximize surface area in the context of thermal design.

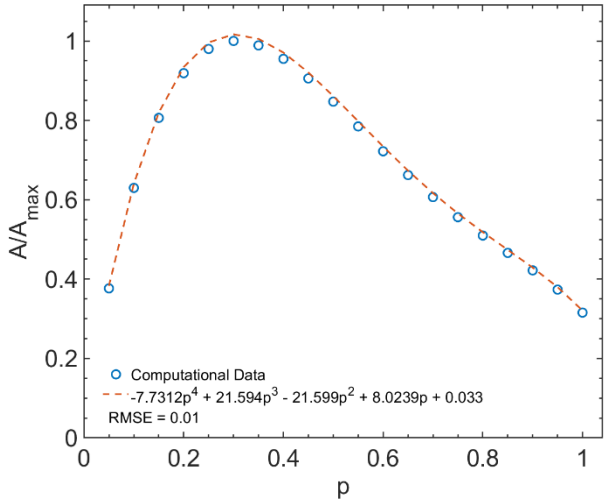

Figure 9. Scaled (with respect to A_{max}) iso-value surface area that is varied with respect to p, as based on Eq. (5).

From the perspective of advanced manufacturing and thermal system design, Eq. (4) and Eq. (5) provide clarity on trends of area generated by the iso-value surface at values of p above and below 1. The reader should note that the identified quantitative relationships apply only to zero-thickness surfaces. For instance, a finite wall thickness common to advanced manufacturing in the range of 1 mm – 3 mm will notably reduce the available area for heat transfer applications. However, realistic wall roughness is expected to create friction with flow and induce perturbations in the boundary layer, benefiting thermal mixing; this aspect remains to be studied in continuing work. Figure 10 illustrates iso-value surfaces generated using data in Figure 8 for representative values of p ranging from 0.01 to 1.0.

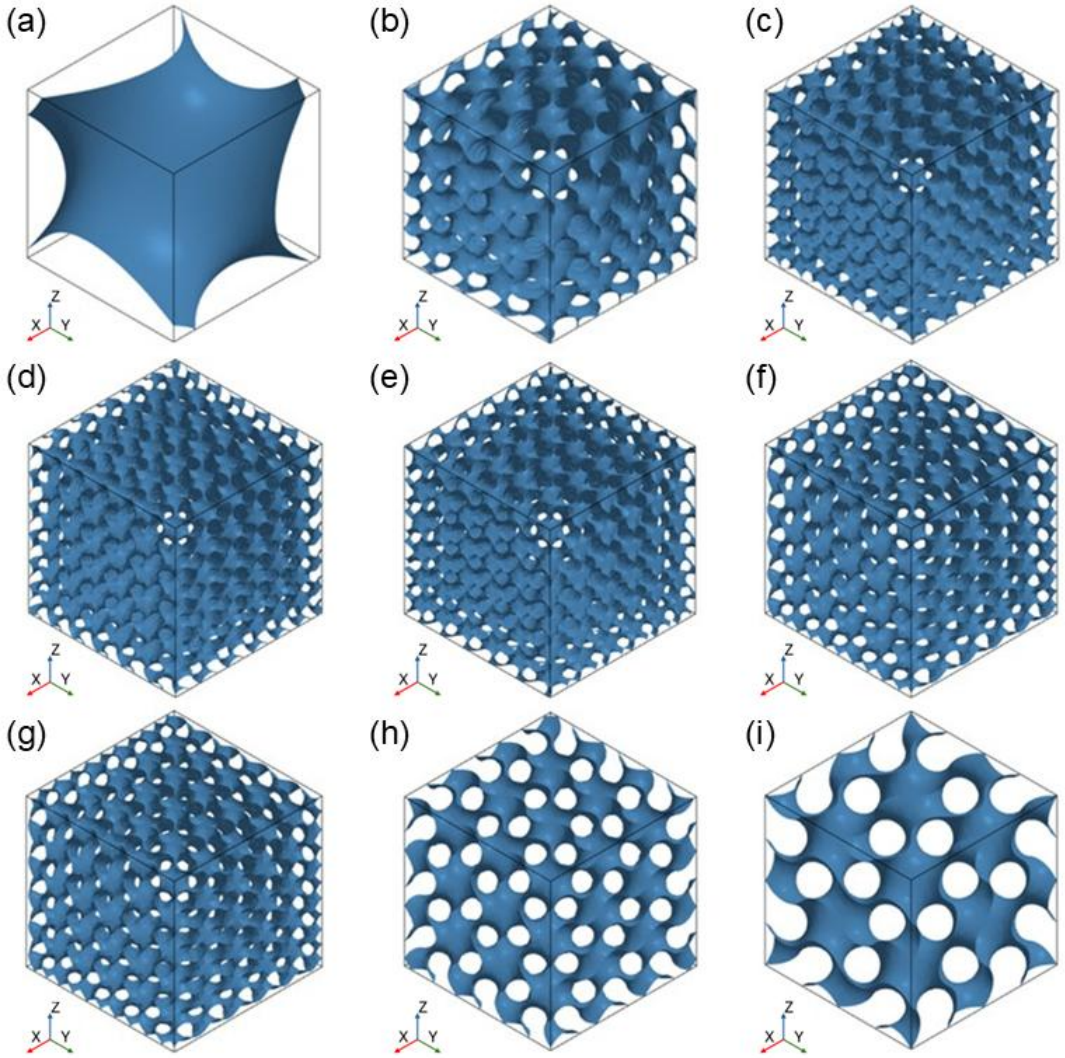

Figure 10. Illustrations of iso-value surfaces for p values of (a) 0.01, (b) 0.1, (c) 0.2, (d) 0.3, (e) 0.4, (f) 0.5, (g) 0.6, (h) 0.8, and (i) 1.0.

A deeper interpretation of computed data in this study is made available through Figure 11. Plot (a) reveals the variation of area with respect to changes in p for fixed values of f and L. The size of the data bubble grows with value of f and the color bar transitions from red to blue as the

value of L increases from 0.003175 m to 0.0254 m; values of the latter have been rounded to three significant figures. Further to the maximum identified by Eq. (5), it is seen that the characteristic gyroid generated at $p = 1$ bears area less than even $p = 0.05$. In future work, it remains to be seen if more than one maximum exists, and at values of p less than 0 and above 2. At larger values of L, fixed values of f and p render larger values of surface area, which is solely attributed to the larger size of the unit cell. In addition, a large value of L complemented by a low value of f will generate the maximum area at a given value of p. This is further corroborated by the qualitative trends evident in figures 11 (b) and (c).

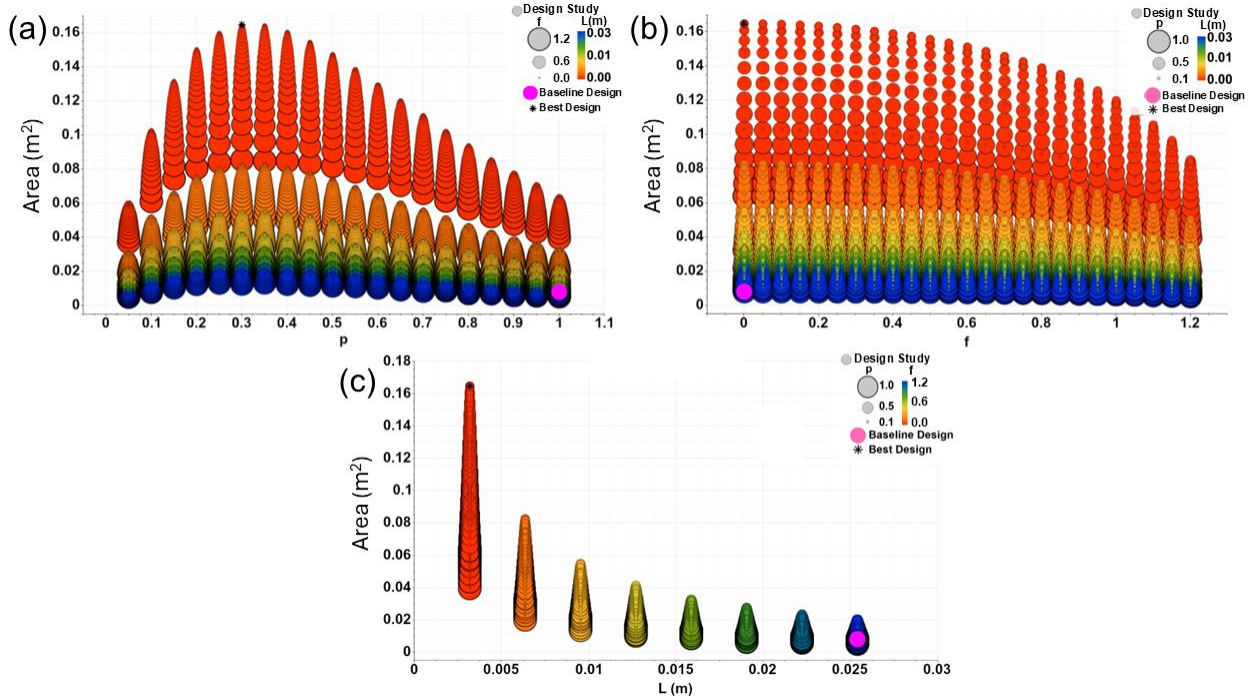

Figure 11. Plot illustrating the variation in iso-value surface area with respect to (a) p, (b) f, and (c) L.

4. Conclusions

The gyroid as a TPMS has received widespread attention due to inherent scalability and periodic surfaces which offer opportunities for customization into numerous end applications. This study provided a summary of recent influential work in the field with a focus on heat transfer applications. The study identified prior work which has laid the foundation to characterize void space in the gyroid, as well as pathways to design new gyroids towards enhanced heat transfer in a compact footprint. The study presented a novel approach towards generating novel shapes of gyroids with the sole objective of maximizing the heat transfer area in comparison to traditional approaches which relied on the fixed unit cell sizes rendered by the characteristic equation of a gyroid.

The study presented the parametric form of the characteristic equation of a gyroid which was adopted in prior research as well but demonstrated the effect of rigid changes in the size of

the unit cell and the number of unit cells within a fixed length towards harnessing greater surface area in a fixed volume. In the context of heat transfer, a key feasibility criterion for design is manufacturability and mechanical integrity. Through rigid manipulation, it was shown that global changes in the unit cell could be implemented which in conjunction with prior research, could develop greater than characteristic surface area. However, this approach leads to abrupt changes in hydraulic profiles due to large changes in cross-sectional area and hydraulic diameter, which are further associated with undesired changes in pressure differential. The novel approach proposed seeks to mitigate these occurrences by providing growth and shrinkage through targeted manipulation of new parameters along the Cartesian co-ordinate system. In doing so, the gyroid gradually grows and shrinks.

Investigation of the effect of the new parameter, p, on the growth of unit cells revealed several inferences. First, at $p = 1$, the characteristic equation was reproduced. At $p > 1$, the area rendered by the gyroid was lower than that of the characteristic value. At $p < 1$, a maximum was identified for a fixed value of n and L. A parametric study was conducted to identify this value, and a maximum in area was identified at $p = 0.3$. A comparison with theory was conducted to compute the exact derivative, and the corresponding maximum was found to be for $p = 0.304857$. Thus, the blind study was verified by the derived analytical value.

Acknowledgements

This manuscript has been authored by UT-Battelle, LLC, under contract DE-AC05-00OR22725 with the US Department of Energy (DOE). The US government retains and the publisher, by accepting the article for publication, acknowledges that the US government retains a nonexclusive, paid-up, irrevocable, worldwide license to publish or reproduce the published form of this manuscript, or allow others to do so, for US government purposes. DOE will provide public access to these results of federally sponsored research in accordance with the DOE Public Access Plan (https://www.energy.gov/doe-public-access-plan). This research was funded by the U.S. Department of Energy, Office of Energy Efficiency and Renewable Energy – Building Technologies Office.

Data Availability

The data that support the findings of this study are available from the corresponding author upon reasonable request.

References

[1] A.H. Schoen, Infinite periodic minimal surfaces without self-intersections, National Aeronautics and Space Administration1970.
[2] K. Große-Brauckmann, W. Meinhard, The gyroid is embedded and has constant mean curvature companions, Calculus of Variations and Partial Differential Equations 4(6) (1996) 499-523.
[3] P.J. Gandy, J. Klinowski, Exact computation of the triply periodic G (Gyroid') minimal surface, Chemical Physics Letters 321(5-6) (2000) 363-371.

[4] J. Owens, C. Daniels, A. Nicolaï, H. Terrones, V. Meunier, Structural, energetic, and electronic properties of gyroidal graphene nanostructures, Carbon 96 (2016) 998-1007.
[5] L. Wallat, P. Altschuh, M. Reder, B. Nestler, F. Poehler, Computational design and characterisation of gyroid structures with different gradient functions for porosity adjustment, Materials 15(10) (2022) 3730.
[6] N. Sathishkumar, K. Kumar, R. Selvam, A. Udayakumar, Optimization of energy absorption and vibration behaviour of TPMS Schwarz P and Schoen Gyroid lattice structures using Taguchi L9 orthogonal array, Journal of Elastomers & Plastics 56(5) (2024) 539-576.
[7] S. Demir, A. Temiz, F. Pehlivan, The investigation of printing parameters effect on tensile characteristics for triply periodic minimal surface designs by Taguchi, Polymer Engineering & Science 64(3) (2024) 1209-1221.
[8] D. Mahmoud, S.R.S. Tandel, M. Yakout, M. Elbestawi, F. Mattiello, S. Paradiso, C. Ching, M. Zaher, M. Abdelnabi, Enhancement of heat exchanger performance using additive manufacturing of gyroid lattice structures, The International Journal of Advanced Manufacturing Technology 126(9) (2023) 4021-4036.
[9] K. Yan, H. Deng, Y. Xiao, J. Wang, Y. Luo, J. Yan, Influence of polishing process on surface morphology and thermo-hydraulic performance of additively manufactured Gyroid-structured heat exchanger, Applied Thermal Engineering 253 (2024) 123828.
[10] L. Dassi, S. Chatterton, P. Parenti, P. Pennacchi, Gyroid lattice heat exchangers: Comparative analysis on thermo-fluid dynamic performances, Machines 12(12) (2024) 922.
[11] M. Beer, R. Rybár, Numerical Study of Fluid Flow in a Gyroid-Shaped Heat Transfer Element, Energies 17(10) (2024) 2244.
[12] B. Jena, V.D. Choudhari, G.S. Kumar, K.A. Prakash, Numerical investigation of gyroid heat exchanger, Journal of Physics: Conference Series, IOP Publishing, 2024, p. 012176.
[13] E. Daifalla, S. Shahpar, I. Tristanto, M. Carta, Multidisciplinary Optimization of Gyroid Topologies for a Cold Plate Heat Exchanger Design, Journal of Engineering for Gas Turbines and Power 146(12) (2024) 121028.
[14] O.-R.L. Guillermo, G.-O. Arturo, P.-B. James, P. Saul, Computational analysis and engineering modeling for the heat transfer and fluid flow through the gyroid TPMS structure, Applied Thermal Engineering 268 (2025) 125865.
[15] R. Attarzadeh, S.-H. Attarzadeh-Niaki, C. Duwig, Multi-objective optimization of TPMS-based heat exchangers for low-temperature waste heat recovery, Applied Thermal Engineering 212 (2022) 118448.
[16] J. Sun, X. Li, H. Mao, Y. Ma, J. Liu, X. Chen, Numerical analysis of the mechanism of porosity effect on the thermal–hydraulic performance of Gyroid-type TPMS structures in combined aero engines, Applied Thermal Engineering (2025) 125453.
[17] Y. Zhang, Y. Yang, G. Chen, Q. Jiang, B. Hao, Analysis of the convective heat transfer performance of multi-morphology lattice structures in thermal management of high-speed aircraft, Physics of Fluids 37(1) (2025).
[18] N. Morselli, M. Puglia, M. Cossu, S. Pedrazzi, A. Muscio, P. Tartarini, G. Allesina, An experimental investigation of indirect evaporative cooling in gyroid-based heat exchangers, Applied Thermal Engineering (2025) 126808.
[19] W. Tang, C. Zou, H. Zhou, L. Zhang, Y. Zeng, L. Sun, Y. Zhao, M. Yan, J. Fu, J. Hu, A novel convective heat transfer enhancement method based on precise control of Gyroid-type TPMS lattice structure, Applied Thermal Engineering 230 (2023) 120797.

[20] W. Tang, J. Guo, F. Yang, L. Zeng, X. Wang, W. Liu, J. Zhang, C. Zou, L. Sun, Y. Zeng, Performance analysis and optimization of the Gyroid-type triply periodic minimal surface heat sink incorporated with fin structures, Applied Thermal Engineering 255 (2024) 123950.
[21] W. Li, G. Yu, Z. Yu, Bioinspired heat exchangers based on triply periodic minimal surfaces for supercritical CO2 cycles, Applied Thermal Engineering 179 (2020) 115686.
[22] M.G. Gado, O. Al-Ketan, M. Aziz, R.A. Al-Rub, S. Ookawara, Triply Periodic Minimal Surface Structures: Design, Fabrication, 3D Printing Techniques, State-of-the-Art Studies, and Prospective Thermal Applications for Efficient Energy Utilization, Energy Technology 12(5) (2024) 2301287.
[23] Siemens, Digital Industries Software: Simcenter STAR-CCM+ design exploration, 2020. https://www.cosmositalia.it/wp-content/softwaredoc/siemens/starccm/Siemens%20SW%20Simcenter%20STAR%20CCM+%20design%20exploration%20Fact%20Sheet.pdf. 2025).
[24] Siemens, Siemens Digital Industries Software: Simcenter STAR-CCM+ 2406 New Features and Enhancements, 2024.